Cambridge Centre for Computational Chemical Engineering

University of Cambridge

Department of Chemical Engineering

Preprint ISSN 1473 – 4273

A combined CFD-population balance approach for multiphase turbulent flows

A. Vikhansky and M. Kraft [1]

submitted: December 14, 2003

[1] Department of Chemical Engineering
University of Cambridge
Pembroke Street
Cambridge CB2 3RA
UK
E-mail: markus_kraft@cheng.cam.ac.uk, av277@cam.ac.uk

Preprint No. 15

c4e

Key words and phrases. Multiphase flows, coalescence/break-up, CFD, Monte Carlo methods.

Edited by
Cambridge Centre for Computational Chemical Engineering
Department of Chemical Engineering
University of Cambridge
Cambridge CB2 3RA
United Kingdom.

Fax: + 44 (0)1223 334796
E-Mail: c4e@cheng.cam.ac.uk
World Wide Web: http://www.cheng.cam.ac.uk/c4e/

Abstract

In the present study we propose an extension of the Euler/Lagrangian approach for liquid-liquid two phase flows when the volume fraction of the dispersed phase is not small. The continuous phase velocity is obtained by solving the Reynolds-averaged Navier-Stokes equations augmented with the turbulence model. Motion of the dispersed phase is calculated by solving the equations of motion taking into account inertia, drag and buoyancy forces. The coupling between the phases is described by momentum source terms and the terms that account for turbulence generation by the droplets' motion. Collision and breakage of the droplets are treated by a single particle Monte-Carlo stochastic simulation method. This method is based on a mass flow formulation and operator splitting technique. For validation of the numerical procedure droplet size distribution and flow fields in a rotating disc contactor are calculated and compared with the existing experimental results.

1 Introduction

Two-phase turbulent liquid-liquid or liquid-gas flows in which a large number of droplets or gas bubbles are dispersed in a continuous phase are frequently found in a variety of chemical and biochemical technological processes. Examples are bubble and extraction columns [17], [2], stirred tanks [28], air-lift reactors [26], amongst others. High interphase area is a very attractive feature for mass transfer operations. Typical applications are encountered in processes involving absorption, extraction, mixing, and emulsification. The dynamics of these systems are dictated by interphase mass, momentum and energy transfer, size distribution of the bubbles/droplets, and generation of turbulence by the dispersed phase.
If the volume fraction of the dispersed phase is not small, breakage, collision and coalescence of the bubbles/droplets, becomes the factor of paramount importance that determines not only size distribution of the dispersed phase but the main hydrodynamical features of both phases. Thus, any adequate computational fluid dynamics (CFD) description of these flows must incorporate droplets population balance as a submodel. Although liquid-liquid dispersion has been numerically investigated in the framework of zero dimensional [28] or multi compartments models [21], there are only very few examples of CFD models that take breakage and coalescence of bubbles into consideration. In [19] an Euler-Euler method has been used to simulate three dimensional two phase flow field in a bubble column. The dispersed phase size distribution was approximated by the introduction of two monosize groups, namely, large bubbles and small bubbles. A more detailed multi-group approximation with a suitable population balance model has been used in [6].
In the present study we use an Euler/Lagrangian approach for calculation of the flow evolving in a rotating disc contactor (RDC). The main advantage of this approach is suitability for treating droplet-droplet and droplet-turbulence interaction in a natural, simple manner. Collisions, coalescence and breakage of the droplets is treated by a Monte Carlo stochastic simulation [27], [12] based on the single-particle method. The model does not require any information on the location and motion of nearby droplets, instead a fictitious collision partner with a given size and velocity is generated. The main drawback that limited applicability of this method in the past is that for each control volume the particle joint size and velocity distribution function have to be sampled and stored. In the present study we applied a discrete representation of the distribution function that requires only small memory resources and allows fast updating.

2 Rotating disc contactor and two phase hydrodynamics model

In this study we simulate two-phase turbulent flow in a pilot-scale RDC [20], its schematic view and flow patterns are given in Fig.1. The device has five compartments, its internal diameter is $150mm$ and diameter of the rotating shaft is $54mm$.

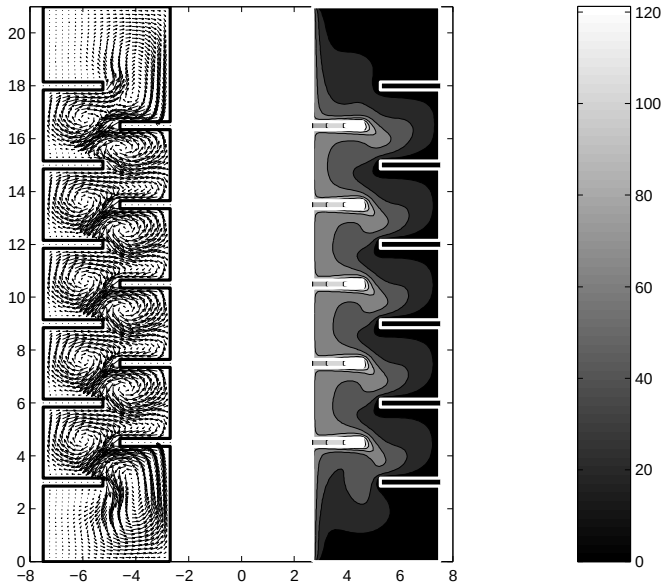

Figure 1: *Schematic view of the rotating disc contactor and flow patterns. Vector plot of the radial and axial velocities in the azimuthal section (left) and contour plot of the azimuthal velocity (right).*

The external diameter of the discs and the internal diameter of the baffles are $92mm$ and $105mm$, respectively. The angular velocity of the shaft Ω_s varies from $150rpm$ to $300rpm$. The continuous phase that has higher density $\rho_c = 0.998g/cm^3$ is supplied from above with volume flux $Q_c = 50 - 100l/hr$, i.e., the average downward velocity is less than $0.18cm/s$, which is several orders of magnitude less than the local velocities encountered in the system. Due to the rotation of the discs the fluid is centrifuged outward in the radial direction and after impinging on the outer wall is reflected inwards. Thus a staggered chain of vortices is formed along the column as is depicted in Fig. 1.

The dispersed (lighter) phase with density $\rho_d = 0.881g/cm^3$ is supplied through the bottom of the column with volume flux $Q_d = 50 - 100l/hr$. Initially, the volume of the droplets is distributed according to a cumulative distribution function $F_{in}(v)$, as the droplets move through the RDC, the distribution changes due to coalescence and breakage. The droplets rise up but are trapped in each compartment by the vortices which play the role of partially mixed reactors.

Generally speaking, the buoyancy forces due to the presence of the lighter phase should make the flow time-dependent and three-dimensional, this considerably complicates numerical treatment of such a flow. In the present study we assume that the agitation in RDC is strong enough and that buoyancy forces are of marginal importance only, and an axisymmetric steady model of the flow is adopted. Thus, we use an iterative solution procedure that is common in many CFD methods, namely, we

solve the Reynolds-averaged Navier-Stokes equations for the continuous phase and then droplets are tracked through the calculated flow field. The source terms that account for the effect of the dispersed phase on the continuous phase are updated and substituted into the Navier-Stokes equations. This procedure is repeated until convergence is achieved.

2.1 Continuous phase hydrodynamics

The fluid flow was calculated by solving the steady Navier-Stokes equations augmented with $k-\varepsilon$ model of turbulence. The model was modified to account for the effect of the droplets on the flow field and turbulence generation. The Reynolds stress tensor σ_R is given by

$$\sigma_{Rij} = \frac{2}{3}\phi_c k\delta_{ij} - \phi_c\nu_t\left(\frac{\partial u_i}{\partial x_j} + \frac{\partial u_j}{\partial x_i} - \frac{2}{3}\frac{\partial u_k}{\partial x_k}\delta_{ij}\right). \tag{1}$$

In the above equations δ_{ij} is the Kronecker delta, ϕ_c is the volume fraction of the continuous phase, and $\vec{u}$ is the mean velocity of the continuous phase. Effective viscosity in the turbulent flow is a sum of molecular and eddy viscosities:

$$\nu_t = \nu + C_\mu k^2/\varepsilon,$$

where $C_\mu = 0.09$. Thus, the equations of conservation of mass, momentum, kinetic energy of turbulence k, and dissipation rate ε reads:

$$\begin{aligned}
\frac{\partial \phi_c u_i}{\partial x_i} &= 0,\\
\frac{\partial \phi_c u_i u_j}{\partial x_j} &= -\frac{\phi_c}{\rho_c}\frac{\partial p}{\partial x_i} - \frac{\partial \sigma_{Rij}}{\partial x_j} - \phi_c g_i + S_{ui},\\
\frac{\partial \phi_c u_i k}{\partial x_i} &= \frac{\partial}{\partial x_i}\left(\frac{\phi_c\nu_t}{\sigma_k}\frac{\partial k}{\partial x_i}\right) + \phi_c(G-\varepsilon) + S_k,\\
\frac{\partial \phi_c u_i \varepsilon}{\partial x_i} &= \frac{\partial}{\partial x_i}\left(\frac{\phi_c\nu_t}{\sigma_\varepsilon}\frac{\partial \varepsilon}{\partial x_i}\right) + \phi_c\frac{\varepsilon}{k}(C_1 G - C_2\varepsilon) + S_\varepsilon.
\end{aligned} \tag{2}$$

In Eqs. (2) p is the pressure that is shared by all the phases, $\vec{g}$ is the acceleration of gravity and $S_{(\cdot)}$ denotes a source of corresponding property due to the presence of the dispersed phase. G is the generation of kinetic energy of turbulence:

$$G = \frac{\nu_t}{2}\left(\frac{\partial u_i}{\partial x_j} + \frac{\partial u_j}{\partial x_i} - \frac{2}{3}\frac{\partial u_k}{\partial x_k}\delta_{ij}\right)^2.$$

The other parameters are constants: $\sigma_k = 1.0$, $\sigma_\varepsilon = 1.3$, $C_1 = 1.44$, $C_2 = 1.92$. In the second of Eqs. (2) we rewrite the source term as $\vec{S_u} := \vec{S_u} - (1-\phi_c)\nabla p$, that accounts for all the forces that the continuous phase exerts on the dispersed phase. After rearrangement of the corresponding terms the momentum conservation reads:

$$\frac{\partial \phi_c u_i u_j}{\partial x_j} = -\frac{1}{\rho_c}\frac{\partial p}{\partial x_i} - \frac{\partial \sigma_{Rij}}{\partial x_j} - \phi_c g_i + S_{ui}.$$

Eqs. (2) are solved on a rectangular mesh by a finite volume method. The diffusive and convective terms are discretised using second-order central-difference and upwind schemes respectively. The boundary conditions are treated by an immersed boundaries method [13]. The iterative procedure for the solution of the resulting set of equations is based on the SIMPLE procedure for pressure correction [23].

2.2 Dispersed phase tracking and interphase interaction

An analogy between chaotic droplets' motion in turbulent flow and motion of molecules in a gas enables application of the methods previously developed for rarefied gas dynamics [5], [16] to population balance of droplets. The direct simulation Monte Carlo (DSMC) method can be formulated as follows. The flow volume is divided into cells. Provided that the droplets' sizes, velocities and positions are known at a time t, the droplets' distribution at time $t + \Delta t$ can be calculated in two steps (operator-splitting technique). The particles are allowed to move, without collision with each other, during the time interval Δt. At the second stage spatially homogeneous coagulation and breakage are sampled randomly in each cell. In this step, a droplet can collide only with those particles that are in the same cell irrespective of the relative positions of the particles within the cell.
In the framework of the Lagrangian method accepted in the present study, each droplet that is tracked through the computational domain represents a group of identical droplets with total volume flux Q_i, i.e., $\sum Q_i = Q_d$. The equations of motion of the droplet read

$$\begin{aligned} \frac{d\vec{x}_d}{dt} &= \vec{u_d}, \\ \frac{d\vec{u}_d}{dt} = \frac{3\rho_c}{4\rho_d D} C_D |\vec{V_c} - \vec{u_d}|(\vec{V_c} - \vec{u_d}) &+ \vec{g}(1 - \frac{\rho_c}{\rho_d}) \\ + \frac{\rho_c}{2\rho_d}(\frac{D\vec{u_c}}{Dt} - \frac{d\vec{u_d}}{dt}) &+ \frac{\rho_c}{\rho_d}\frac{D\vec{u_c}}{Dt}. \end{aligned} \tag{3}$$

Here $\vec{x}_d$, $\vec{v}_d$ and D are the position, velocity and diameter of the droplet respectively. The terms on the right hand side of Eq. 3 represent drag, buoyancy, added mass and pressure forces, respectively, [17]. $\vec{V_c} = \vec{u}_c + \vec{v'}$ is the instantaneous velocity of the ambient continuous phase that consists of the mean time-independent part and a turbulent pulsation. The drag coefficient C_D is calculated from the empirical correlation:

$$C_D = \begin{cases} 24Re^{-1}(1 + 0.15Re^{0.687}) & Re \leqslant 1000, \\ 0.44 & Re > 1000, \end{cases}$$

where $Re = D|\vec{V_c} - \vec{u}_d|/\nu$.
The above described momentum balance for the dispersed phase does not contain momentum transfer due to droplet-droplet interaction. The attempt to treat momentum interchange through inelastic binary collisions leads to so-called *clustering instability* [9], i.e., formation of regions with high concentration of the dispersed

phase and, in the case of droplets, formation of one large drop. This phenomenon has never been observed in an experiment. Note, that the theory of hydrodynamic interaction in dense suspensions is far from being resolved and the assumption of binary collision cannot be applied in this case. Thus, in the present investigation we do not include momentum transfer in the collision process and model droplet-droplet force interaction through a mean field approach, i.e., correct the drag coefficient by a ϕ_c^2 factor as was done in [6], [14].
The mean part of the instantaneous fluid velocity is linearly interpolated from the neighbouring grid nodes, while the fluctuating component $\vec{v'}$ is randomly generated according to the turbulent Langevin model [27].
Consider a droplet and the ambient liquid envelope (Fig. 2). At time t and the point O the fluctuating component of fluid velocity is $\vec{v'}(t, O)$. At the next moment of time $t + \Delta t$ the liquid particle is advected by the mean flow to the point $O' = O + \Delta t \vec{u}_c$. The fluctuation at time $t + \Delta t$ is correlated with that in the previous one. We used an exponential approximation of the Lagrangian correlation function

$$\frac{\langle v_i'(t) v_j'(t + \Delta t)\rangle}{\langle v'^2\rangle} = R_L(\Delta t)\delta_{ij} = \exp(-\frac{\Delta t}{T_L})\delta_{ij},$$

where $T_L = C_T(2/3)k\varepsilon^{-1}$ is the time scale of the turbulence, and $C_T = 0.4$.
In the same moment in time $t + \Delta t$ the droplet is at the new point $O'' = O + \Delta t \vec{u}_d$. The correlation for two points O' and O'' is given by the Eulerian correlation tensor

$$\frac{\langle v_i'(O') v_j'(O'')\rangle}{\langle v'^2\rangle} = R_{ij}^E(\vec{r}) = [f(r) - g(r)]\frac{r_i r_j}{r^2} + g(r)\delta_{ij},$$

which is a function of the vector $\vec{r}$ connecting these two points, and where $r = \|\vec{r}\|$. The functions $f(r)$ and $g(r)$ are longitudinal and transversal (with respect to the vector $\vec{r}$) correlation coefficients. Since the liquid is incompressible $f(r)$ and $g(r)$ are related through the continuity equation $dg(r)/dr = f(r) + (r/2)df(r)/dr$. In the present study we use the following approximation for the correlation coefficients [27], [31]:

$$f(r) = \exp(-\frac{r}{L_E}),$$
$$g(r) = (1 - \frac{r}{2L_E})\exp(-\frac{r}{L_E}),$$

where $L_E = \sqrt{2/3k}T_L$ is the spatial correlation length. Eventually, the longitudinal and transversal components of fluctuation velocity are

$$v_n'(t + \Delta t, O'') = R_L f v_n'(t, O) + \sqrt{1 - (R_L f)^2}\xi,$$
$$v_t'(t + \Delta t, O'') = R_L g v_t'(t, O) + \sqrt{1 - (R_L g)^2}\xi,$$

where ξ is a Gaussian random number with zero mean value and standard deviation equal to the mean-square velocity of the vortices that contribute to the motion of the droplet. In order to estimate the dispersion of ξ we need to take into account that

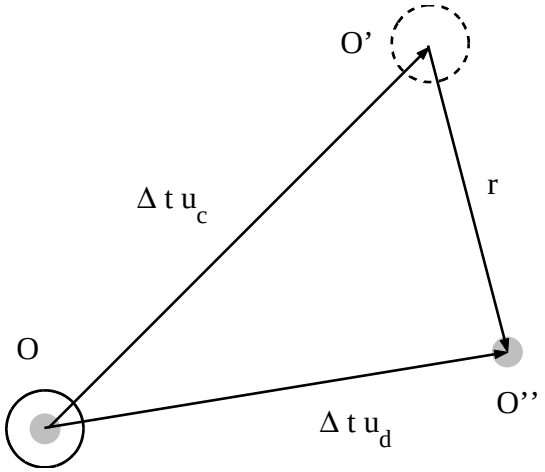

Figure 2: *A droplet (gray) and the ambient liquid particle in turbulent flow.*

a droplet is advected by turbulent vortices that are larger than the diameter of the droplet. Since spectral energy density in the inertial subrange is $E(\lambda) = 1.7\varepsilon^{2/3}\lambda^{-5/3}$ the mean-square velocity of these vortices is (see [4])

$$\langle \xi^2 \rangle = \frac{2}{3}k - \int_{2\pi/D}^{\infty} E(\lambda)d\lambda \approx \frac{2}{3}k - 0.5(\varepsilon D)^{2/3} \tag{4}$$

Eqs.(3) are solved using a first-order implicit Euler method. The time step of integration Δt has to be chosen smaller than the time scales relevant to motion of the droplet, namely: the time required for a droplet to cross a control volume, relaxation time $\tau_{relax} = 4D(\rho_d/\rho_c + 0.5)/(3C_D|\vec{V_c} - \vec{u_d}|)$ and the time scale of the turbulence T_L.

The effect of the dispersed phase on the fluid flow is calculated by means of a particle-source-in-cell method [17], which considers the droplets as a local source of the momentum, kinetic energy of turbulence and dissipation rate. In the beginning of the n^{th} dispersed phase iteration the *future* volume fraction and sources are set to be 0: $\phi_d^{n+1} := 0$, $S_{(\cdot)}^{n+1} := 0$. During one step of the integration procedure a droplet changes the volume fraction of the dispersed phase ϕ_d^{n+1} in the cell where its centre of gravity is located by $\Delta t Q_i / V_{cell}$, where V_{cell} is the volume of the cell. Thus, the total volume fraction in a cell is obtained by summation of the above formula over all time steps and all droplets that visit the cell during the dispersed phase iteration:

$$\phi_d^{n+1} = \sum \frac{\Delta t Q_i}{V_{cell}}.$$

Following [17] the droplet contribution to the momentum source reads

$$\vec{s_u} = -\frac{\Delta t Q_i \rho_d}{V_{cell}\rho_c}\left(\frac{d\vec{u_d}}{dt} - (1 - \frac{\rho_c}{\rho_d})\vec{g}\right),$$

and the total momentum source due to the presence of the dispersed phase is $\vec{S_u^{n+1}} = \sum \vec{s_u}$, where the summation is over all time steps and all droplets that visit the cell. The production of kinetic energy of turbulence by the chaotic motion of the droplets is

$$S_k^{n+1} = \Sigma(\vec{u_d} \cdot \vec{s_u}) - \vec{u_c} \cdot S_u^{n+1},$$

where the first term is the total work done by the dispersed phase and the second term is the work done by the mean interface force [17]. The source term for ε has the standard form, i.e., it is the ratio between production of kinetic energy and time scale of the turbulence:

$$S_\varepsilon^{n+1} = C_3 \frac{\varepsilon}{k} S_k^{n+1},$$

where $C_3 = 1.8$. In the end of the dispersed phase iteration we underrelax the source terms and volume fraction as $S_{(\cdot)}^{n+1} = cS_{(\cdot)}^{n+1} + (1-c)S_{(\cdot)}^{n}$, where $c = 0.3 - 0.4$.

3 Breakage, collision and coalescence of the droplets

3.1 Breakage rate and distribution of the resulting daughter droplets

According to the common view on the fragmentation of bubbles and droplets in turbulent flows, a droplet breaks if the dynamic pressure due to the turbulence exceeds the pressure due to surface tension, while the mechanisms that govern the size distribution of the resulting daughter droplets are less clear. In the present investigation we assume that the characteristic size of the fragments is also dictated by the balance between the surface tension and the dynamic pressure of the vortices that are smaller than the diameter of the daughter particle D_d [22]. The surface pressure of the daughter drop is $\tau_s(D_d) = 6\sigma/D_d$, where σ is the surface tension. The dynamic pressure of the turbulence at the scale of the parent drop $\tau_t(D)$ is exponentially distributed with parameter

$$\frac{1}{2}\rho_c \overline{\Delta u^2(D)} = \frac{1}{2}\beta\rho_c(\varepsilon D)^{2/3}, \tag{5}$$

where $\overline{\Delta u^2(D)}$ is the characteristic velocity difference between two points separated by distance D, and the constant $\beta = 8.2$ was given by Batchelor [4]. We assume that the dynamic pressure of the turbulence at the scale of the daughter drop D_d scales according to Kolmogorov's universal scaling, i.e., $\tau_t(D_d) = (D_d/D)^{2/3}\tau_t(D)$. The equation $\tau_s(D_d) = \tau_t(D_d)$ yields

$$D_d = \Big(\frac{6\sigma D^{2/3}}{\tau_t(D)}\Big)^{3/5}. \tag{6}$$

We now simulate breakage as follows:

1. Dynamic pressure of the turbulence $\tau_t(D)$ is generated exponentially with parameter (5).

2. Minimum possible size of daughter drop is calculated according to Eq. (6).

3. Number of the fragments N_d is the integer part of the fraction $(D/D_d)^{1/3}$.

4. If $N_d < 2$ breakage does not occur, otherwise we create $N_d - 1$ droplets with diameter D_d, while the rest of the mass remains in the droplet with diameter $D'_d = (D^3 - (N_d - 1)D_d^3)^{1/3}$.

The time that is necessary for breakage can be estimated as the life time of the turbulent vortex with size D:

$$\frac{1}{t_{break}} = \frac{\sqrt{\overline{\Delta u^2(D)}}}{D} = \sqrt{\beta}\frac{\varepsilon^{1/3}}{D^{2/3}}. \tag{7}$$

3.2 Coalescence rate

Since during the collision step we assume a uniform distribution of the droplets inside a cell, the probability that two particles that are in the same spatial cell and have sizes and velocities D_i and $\vec{u}_i$, respectively, can collide during a time interval Δt is

$$h_{1,2}\Delta t = \frac{\pi}{4}\chi(\phi_d)(D_1 + D_2)^2|\vec{u}_1 - \vec{u}_2|\sqrt{1 - f^2(\frac{D_1 + D_2}{2})}\frac{\Delta t}{V_{cell}}, \tag{8}$$

where $h_{1,2}$ is the collision rate and $\chi(\phi_d)$ is the radial distribution function

$$\chi(\phi_d) = \frac{1 - \phi_d/2}{(1 - \phi_d)^3}.$$

In Eq. (8), unlike in classical statistical mechanics, the relative velocity is reduced by the factor $\sqrt{1 - f^2((D_1 + D_2)/2)}$ that accounts for the longitudinal correlation between two points in turbulent flow that are separated by the distance $(D_1 + D_2)/2$. As the droplets approach each other they do not necessarily merge, a liquid film separates the droplets and plays the role of a barrier that prevents immediate coalescence. Since the droplets are not rigid particles but have a finite elasticity due to surface tension, the time of contact between two droplets is non-zero. Thus we adopt the following model for the droplets' interaction: if the time of contact $t_{contact}$ is less then the time that is necessary for drainage of the barrier liquid film $t_{drainage}$, then the colliding droplets do not coalesce, otherwise they merge into a single drop. The equation for the coagulation rate of the droplets reads

$$K_{1,2} = h_{1,2}H(t_{contact} - t_{drainage}), \tag{9}$$

where $H(\cdot)$ is the Heaviside function.

In the present investigation we follow the analysis of the relative motion of two droplets that was done in [7, 15]. The effective mass (together with added mass) of a droplet with mass m_i is $M_i = m_i(1+0.5\rho_c/\rho_d)$. The reduced mass that characterizes

the inertia of the relative motion is $M = M_1 M_2/(M_1 + M_2)$ (see [18]), while the rigidity of contact is $K = \pi\sigma$ (see [15]). Thus the time of contact can be estimated as a half-period of a pendulum with rigidity K and mass M. Since $t_{contact}$ cannot be higher than the life time of the turbulent vortex with size $(D_1 + D_2)/2$, we choose the contact time to be

$$t_{contact} = \min\left(\pi\sqrt{\frac{M}{K}}, \sqrt{\beta}\frac{2^{2/3}\varepsilon^{1/3}}{(D_1 + D_2)^{2/3}}\right). \tag{10}$$

The drainage time between two droplets is [7, 15]

$$t_{drainage} = \frac{\rho_c v_{rel}}{4\sigma}\frac{D_1 D_2}{D_1 + D_2}, \tag{11}$$

where v_{rel} is the relative velocity of the droplets at the beginning of the contact.

4 Solution of the population balance model

The computational domain is divided in to around 10^4 cells. Since for a proper representation of the polydispersed droplets ensemble one needs $5 - 15$ droplets in each spatial cell, modelling of the dispersed phase requires simultaneous tracking of about 10^5 droplets. Given the droplets' number density is nonuniform over the flow region, in order to provide the minimum necessary number of droplets in the low-density regions, one needs to further increase the total number of computational droplets. A significant simplification can be achieved if we use the fact that the flow is steady. A single particle (or alternatively, test particle) method (SPM) can be applied. The spatially homogeneous coagulation/fragmentation step does not require any information about neighboring particles, instead a particle (that is referred to as test particle) coagulates with a fictitious collision partner that is generated according to the local particles' distribution [27], [12], thus, the particle always has a collision partner even in a low-density region. As soon as the particle leaves the system, the new particles' distribution function is recalculated. This procedure is iterative until convergence is achieved. Note that the coagulation SPM step naturally fits the general iterative strategy adopted in the present investigation and the iterative nature of the above method should not be considered as a drawback. The SPM for the Boltzmann equation has a longer history than the DSMC method [11]. Recently this method has been applied for spatially homogeneous coagulation-fragmentation problems [24], [25]. The main obstacle that limited wide application of SPM in the past was the necessity to store and update the particle distribution function in each cell of the computation domain. This difficulty has been resolved by Vlasov [30]. According to this approach only the particles' number density and the parameters of a few (maybe even one) particles are stored in each cell. These particles are referred to as field (or target) particles. When a test particle crosses a cell, one of the field particles is replaced by the test particle with a probability p

that is proportional to the residence time t_{res} of the test particle in the cell.
The spatially homogeneous coagulation-fragmentation equation reads:

$$\frac{\partial n(t,x)}{\partial t} + \frac{n(t,x)}{\theta(x)} - \frac{N_{in}(x)}{V_{cell}} = - \int_0^\infty K(x,x')n(t,x')n(t,x)dx' - g(x)n(t,x) - \frac{1}{2}\int_0^x K(x-x',x')n(t,x')n(t,x-x')dx' + \int_x^\infty g(x')\beta(x,x')n(t,x')dx'. \quad (12)$$

In the above equation $n(t,x)$ is the number density of the droplets that have volume x at time t. The droplets that enter the cell are distributed according to $N_{in}(x)$, and $\theta(x)$ is a size-dependent residence time. The probability that two droplets with volumes x and x', respectively, coalesce during a small time interval dt is $K(x,x')dt$. The collision probability depends on the relative velocity between the two droplets (c.f. Eqs. (8) - (9)) but we omit it from the above formula for the sake of simplicity. A droplet breaks during a small time interval dt with probability $g(x)dt$, and the number of fragments with size x that are formed from one droplet with volume x' is $\beta(x,x')$.
Let us reformulate Eq. (12) in terms of mass density (so-called mass flow formulation [1, 8, 10]). The mass density of the droplets that have volume x at a time t is $m(t,x) = xn(t,x)$, and $M_{in}(t,x) = xN_{in}(t,x)$. In order to reformulate the coagulation equation (12) in terms of $m(t,x)$, we express $n(t,x)$ as $m(t,x)/x$, substitute it into Eq. (12) and multiply the equation by x. Note, that if $K(x,x') = 0$ for $x \leqslant 0$ or $x' \leqslant 0$, and $\beta(x,x') = 0$ for $x' < x$ the limits of integration in (12) can be extended from $-\infty$ to ∞. After some algebra we obtain [25, 1, 8]:

$$\frac{\partial m(t,x)}{\partial t} + \frac{m(t,x)}{\theta(x)} - \frac{M_{in}(x)}{V_{cell}} = - \int \frac{K(x,x')}{x'}\mu(t,x')m(t,x)dx' - g(x)m(t,x) + \int \frac{K(x-x',x')}{x'}\mu(t,x')m(t,x-x')dx' + \int g(x')\frac{\beta(x,x')x}{x'}m(t,x')dx', \quad (13)$$

where $\mu(t,x)$ is the mass density of field particles that converges to the mass density of test particles $m(t,x)$ as $t \to \infty$. The factor of $1/2$ before the first integral in Eq.(12) disappears because coagulation reduces the number of droplets but does not affect their volumes.
The Monte Carlo algorithm for the single particle process is as follows. As it was mentioned above, the dispersed phase iteration consists of sequential tracking of the number of droplets. We represent the field droplets ensemble at the beginning of the n^{th} particle tracking by N target droplet groups with volumes $y^n = (y_1^n, ..., y_i^n, ..., y_N^n)$ and velocities $\vec{v}^n = (\vec{v}_1^n, ..., \vec{v}_i^n, ..., \vec{v}_N^n)$. The volume of the i^{th} group is ϕ_d/N and the number of droplets in the group is $\phi_d/(Ny_i^n)$. Since the probability that during a small time interval dt the test droplet collides with one field droplet from the i^{th} group is $h(x,y_i^n)dt$ (c.f. Eq. (8)), the probability that the test droplet collides with

any of the i^{th} field droplets is $h(x, y_i^n)(\phi_d/y_i^n)dt$. Thus, the collision rate ρ of the test droplet is given by a summation of the above formula over all groups of target droplets:

$$\rho = \frac{\phi_d}{N} \sum_{i=1}^{N} \frac{h(x, y_i^n)}{y_i^n}. \tag{14}$$

We sample breakage of the test droplet with rate $1/t_{break}$ which is calculated according to Eq. (7).
At the beginning of the simulation we initialize some target droplet distribution y^0 and then the simulation algorithm reads:

1. Set $y^{n+1} = y^n$ and $\vec{v}^{n+1} = \vec{v}^n$.

2. Set time counter $t_{count} = 0$.

3. Generate an exponentially distributed time increment τ with parameter $\rho + 1/t_{break}$, update the time counter as $t_{count} = t_{count} + \tau$.

4. With probability
$$\alpha \frac{\tau Q_i}{\phi_d V_{cell}} \tag{15}$$
replace a uniformly chosen y_i^{n+1} by x and $\vec{v}_i^{n+1}$ by $\vec{u}_d$, where α is a constant.

5. With probability $\rho(x)/(\rho(x) + 1/t_{break})$ choose coagulation step, overwise go to step 8.

6. Choose collision partner according to the distribution
$$\frac{h(x, y_i^n)\phi_d}{N\rho y_i^n}. \tag{16}$$

7. Calculate contact time and drainage time according to Eqs. (10) and (11), respectively. If $t_{contact} \geqslant t_{drainage}$ replace x by $x + y_i^n$, otherwise reject the coalescence. Go to step 9.

8. Breakage step. Generate the daughter droplet size D_d and the number of fragments N_d as is described in Eq. (6) and the breakage algorithm. If $N_d \geqslant 2$ replace x by a droplet with diameter D_d with probability $(N_d - 1)(D_d/D)^3$, otherwise replace x by a droplet with diameter D'_d.

9. If $t_{count} \leqslant \Delta t$ go to step 3.

10. Move the droplet according to Eqs. (3). During this step the droplet can pass from one cell to another. If the droplet leaves the system, generate a new $(n+1)^{th}$ droplet at the bottom of RDC according to inlet size distribution $F_{in}(x)$ and go to step 1. If not, go to step 2.

This method has been investigated in previous work [29] and its performance was compared with a direct simulation method in an ideally stirred reactor. The main results are the following.

1. It was shown that both methods provide identical results within similar CPU time.

2. The probability that a test particle will leave a cell without being registered in the field particles' array is given by the product of Eq. (15) over all time steps:
$$\prod_j (1 - \alpha \frac{\tau_j Q_i}{\phi_d V_{cell}}) \approx 1 - \alpha \frac{Q_{in}}{\Phi^n V} \sum_j \tau_j = 1 - \alpha \frac{Q_i}{\phi_d V_{cell}} t_{res}, \qquad (17)$$
where t_{res} is a characteristic residence time of a droplet in the cell. In the above formula we used the assumption that $\tau \ll t_{res}$. Since $\phi_d \sim n_d Q_i t_{res}/V_{cell}$, (where n_d is the number of droplets that crossed the cell), in order to keep the probability (17) positive one needs $\alpha \approx 1$ if each cell is visited by more then one computational droplet during the dispersed phase iteration. In the present investigation we used $\alpha = 0.5$.

3. The numerical experiments reveal that in order to avoid correlation between consecutive collisions, one needs the number N of field droplets to be approximately equal to the number of collisions that a test droplet undergoes before it leaves the cell. In usual CFD applications the size of control volumes is chosen in such a way that the probability of more than one collision in one cell is small, even one field particle per cell can be sufficient. To calculate the results presented below we used from 6 to 12 field droplets per cell.

5 Results and discussion

There are two main forces that govern the flow field in a RDC, namely, inertia forces due to rotation of the discs and dispersed phase buoyancy forces. In the absence of the less dense dispersed phase the velocity field consists of a chain of 10 staggered vortices, a vortex between two discs and a counterrotating vortex between two baffles, etc., as is depicted in Fig. 3. This picture persists for all values of Ω_s. These vortices trap the droplets and significantly slow down the rising velocity of the dispersed phase. Thus, as the droplets accumulate in these regions, a lower average density of the mixture leads to an additional upward directed force that deforms the flow field. The results of the calculations are presented on Figs. 3, 4. When the angular velocity of the shaft is sufficiently high, the dispersed phase decreases the size of the vortices that are below the discs and moves them toward the periphery, but the qualitative structure of the flow does not change. The downward inclined jets that originate from the rotating discs serve as the main obstacle that prevents a droplet transition from one compartment to another and the droplet can be trapped in a compartment for a long time. The typical trajectories are presented in Fig. 5. As

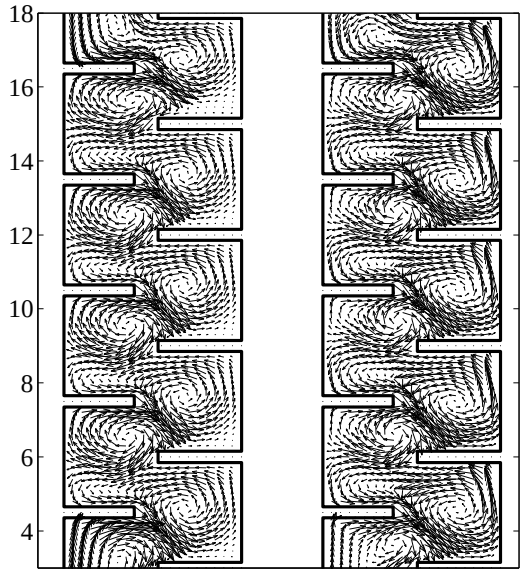

Figure 3: *Vector plot of the radial and axial velocities in the azimuthal section for different volume fractions of the dispersed phase* $\langle \phi_d = 0 \rangle$ *(left) and* $\langle \phi_d = 15\% \rangle$ *(right),* $\Omega_s = 300rpm$.

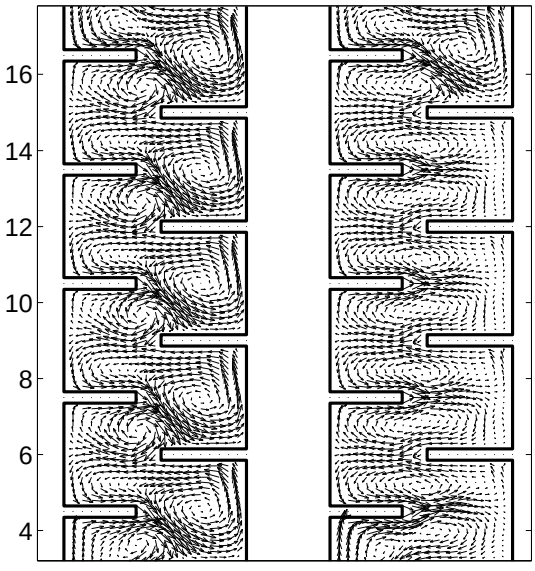

Figure 4: *Vector plot of the radial and axial velocities in the azimuthal section for* $\Omega_s = 300rpm$ *(left) and* $\Omega_s = 200rpm$ *(right),* $Q_c = Q_d = 100l/hr$.

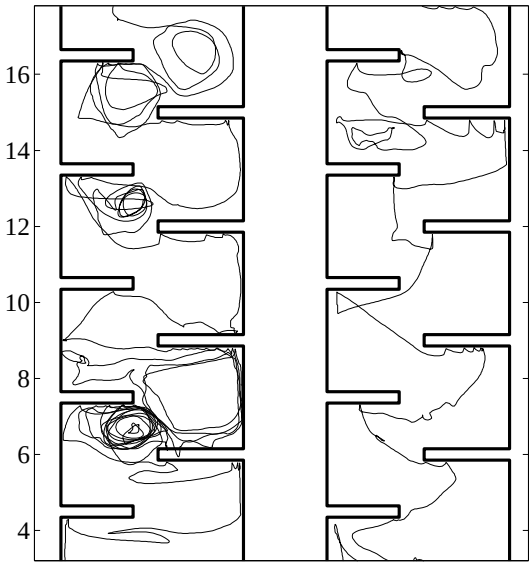

Figure 5: *Typical trajectories of the droplets* $\Omega_s = 300rpm$ *(left) and* $\Omega_s = 200rpm$ *(right),* $Q_c = Q_d = 100l/hr$.

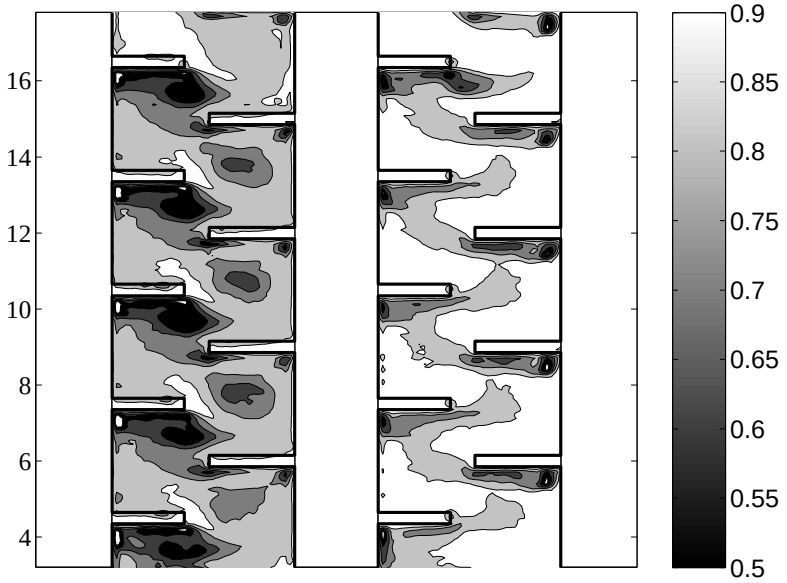

Figure 6: *Volume fraction of the continuous phase in the azimuthal section for* $\Omega_s = 300rpm$*, average hold-up is* 15.0% *(left), and* $\Omega_s = 200rpm$ *(right) average hold-up is* 5.98%*,* $Q_c = Q_d = 100l/hr$.

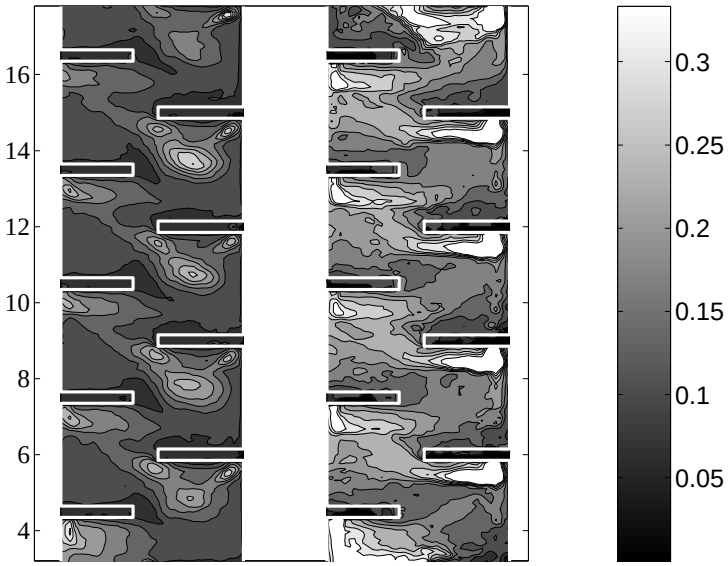

Figure 7: *Mean-mass diameter of the droplets (cm) for $\Omega_s = 300rpm$ (left) and $\Omega_s = 200rpm$ (right), $Q_c = Q_d = 100l/hr$.*

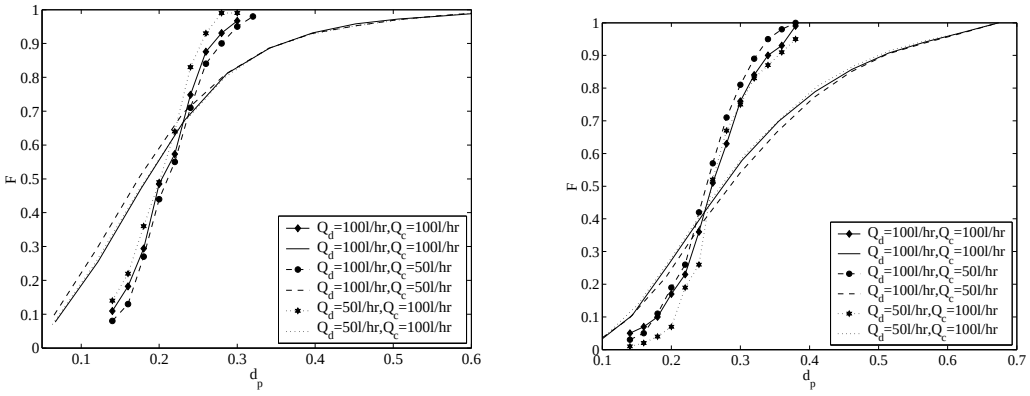

(a) $\Omega_s = 300rpm$ (b) $\Omega_s = 200rpm$

Figure 8: *Calculated (lines) and measured (symbols) cumulative mass distribution function of the droplets diameter d_p (cm) at the outlet.*

the rotation velocity of the shaft decreases the relative importance of the buoyancy forces becomes higher, and for $\Omega_s < 250rpm$ bifurcates to the system of elongated vortices that extend from the shaft to the external wall of the RDC. The jets that separate these vortices are horizontal and do not constitute a serious obstacle for buoyant droplets. Thus the residence time of a droplet in each compartment is less and its trajectory is less tangled.

Two different structures of flowfields lead to different distributions of the dispersed phase inside the contactor (Fig. 6). Since for $\Omega_s = 300rpm$ the characteristic velocity in the azimuthal plane is about $20cm/s$, and given that the characteristic diameter of the vortex is about $1.5cm$, the inertia forces are strong enough in comparison with the buoyancy forces, and the continuous phase accumulates in the centres of the vortices. For lower values of Ω_s the acceleration of gravity is much higher than the centripetal acceleration and the droplets rise up and stick to the discs and, mainly, to the baffles.

It is conceivable that a high concentration of the dispersed phase leads to high collision and coalescence rates, and therefore to a larger characteristic size of the droplets. The distribution of the mass-mean diameter of the dispersed phase is plotted on Fig. 7. Visual comparison of Fig. 6 and Fig. 7 reveals that while for low rotation speeds of the shaft, the patterns of characteristic droplet size follow the volume fraction of the dispersed phase, for $\Omega_s = 300rpm$ the characteristic size of the droplets in the vortices adjacent to the discs is relatively small. The intensive flow and, therefore, high dissipation rate of the turbulence in this region result in a high breakage rate that prevents formation of large droplets.

In order to validate our numerical model we compared the computational predictions with the available experimental data [20], [3]. Cumulative mass distribution functions for the droplets diameter at the outlet are presented in Fig. 8. Notably, both the experiment and the calculations predict that the droplet size distribution does not depends significantly on Q_c and Q_d. As one can see, the predicted mass-mean diameter is close to the measured value, while the computational model overestimates the standard deviation of the distribution approximately by a factor of 3. The fact that the calculated distribution is wider than the distribution in the experiment could be the result of overestimation of the coagulation rate by the model. Since the large drops formed cannot survive in the turbulent flow, high numbers of breakage/coalescence events increases the standard deviation of droplets' diameter. Note that Eqs. (6)-(11) provide only orders of magnitude for the estimated parameters but not *exact* values. These equations are correct up to some coefficients of order one, that have to be identified from the experimental data. Since our model, unlike most of the dispersion models found in the literature, does not contain any fitting parameters, the agreement between the experimental and numerical data is satisfactory.

6 Conclusions

In the present work an Euler/Lagrange formulation has been proposed for the numerical simulation of the dispersion of droplets in two phase turbulent flows. The flow field of the continuous phase was described by the $k - \varepsilon$ Reynolds-averaged Navier-Stokes equations and calculated by a control volume method. The simulation of the dispersed phase by the Lagrangian method requires the solution of a stochastic ordinary differential equation for each drop that represents a cluster of drops with identical properties. The instantaneous fluid velocity at the droplet location consists of the local mean velocity and the random component generated by the Langevin model. The effect of the dispersed phase on the fluid flow is calculated by means of the particle-source-in cell method that considers the droplets as a local source of momentum, kinetic energy and dissipation rate of turbulence. This approach allows simulation of droplets-flow interaction in the most natural way.
Special attention has been given to coagulation and breakage of the droplets, which was treated by a single particle Monte Carlo method. The droplets ensemble was split into test droplets that were tracked through the system and target droplets that were used for generation of a fictitious collision partner. This method is algorithmically simple and does not require extra storage resources as other variants of SPM. The fragmentation of a drop in the turbulent flow field occurs if the dynamic pressure due to turbulence exceeds the pressure due to surface tension. The model for droplet collision is developed in two stages. In the first stage, the collision probability due to relative motion of the droplets is calculated in the manner common in statistical mechanics. In the second, the coalescence occurs if the time that is necessary for drainage of the liquid film separating two droplets is less than the contact time between the droplets. Finally, the results of numerical simulations have been compared with the available experimental data. Although the proposed computational model does not contain any fitting parameters it predicts characteristic size at the outlet of the RDC correctly, but the calculated size distribution is wider than the measured one.

7 Acknowledgement

This work has been supported by the EPSRC (grant number GR/R85662/01) under the title "Mathematical and Numerical Analysis of Coagulation-Diffusion Processes in Chemical Engineering".

References

[1] H. Babovsky. On a monte carlo scheme for smoluchowski's coagulation equation. *Monte Carlo Methods Appl.*, 5:1–18, 1999.

[2] H.-J. Bart. *Reactive extraction.* Springer, 2001.

[3] H.-J. Bart. Reactive extraction of acids or metals - the state of the art of column design. *Chemical Engineering Sci.*, 57:1633 – 1637, 2002.

[4] G. K. Batchelor. *The theory of homogeneous turbulence.* Cambridge University Press, 1956.

[5] G. A. Bird. *Molecular gas dynamics.* Clarendon press, 1976.

[6] V. V. Buwa and V. V. Ranade. Dynamics of gas-liquid flow in a rectangular bubble column: experiments and single/multi-group cfd simulations. *Chemical Engineering Sci.*, 57:4715–4736, 2002.

[7] A. K. Chesters. The modelling of coalescence processes in fluid-liquid dispersions: A review of current understanding. *Trans. IChemE*, 69:259–270, 1991.

[8] A. Eibeck and W. Wagner. Stochastic particle approximation for smoluchovski's coagulation equation. *Ann. Appl. Probab.*, 11:1137–1165, 2001.

[9] I. Goldhirsch and G. Zanetti. Clustering instability in dissipative gases. *Phys. Rev. Lett.*, 70:1619–1622, 1991.

[10] M. Goodson and M. Kraft. Stochastic simulation of coalescence and breakage processes: a practical study. Technical Report 9, c4e-Preprint Series, Cambridge, 2003.

[11] J. K. Haviland and M. L. Lavin. Application of the monte carlo method to heat transfer in a rarified gas. *Phys. Fluids*, 11:1399–1405, 1962.

[12] C. A. Ho and M. Sommerfeld. Modelling of micro-particle agglomeration in turbulent flows. *Chemical Engineering Sci.*, 57:3073–3084, 2003.

[13] G. Iaccarino and R. Verzicco. Immersed boundary technique for turbulent flow simulations. *Appl. Mech. Rev.*, 56:331–347, 2003.

[14] M. Ishii and N. Zuber. Drag coefficient and relative velocity in bubbly, droplet or particulate flows. *AIChE Journal*, 25:843–855, 1979.

[15] A. M. Kamp, A. K. Chesters, C. Colin, and J. Fabre. Bubble coalescence in turbulent flows: A mechanistic model for turbulence-induced coalescence applied to microgravity bubbly pipe flow. *Int. J. Multiphase Flow*, 27:1363–1396, 2001.

[16] A. Kitron, T. Elperin, and A. Tamir. Stochastic modelling of the effects of liquid droplet collisions in impinging streams absorber and combustors. *Int. J. Multiphase Flow*, 17:247–265, 1991.

[17] S. Laín, D. Bröder, M. Sommerfeld, and M. F. Göz. Modelling hydrodynamics and turbulence an a bubble column usin euler-lagrange procedure. *Int. J. Multiphase Flow*, 28:1381–1407, 2002.

[18] L. Landau and E. M. Lifsitz. *Mechanics*. Butterworth-Heinemann, 1976.

[19] F. Lehr, M. Millies, and D. Mewes. Bubble-size distributions and flow fields in bubble columns. *AIChE Journal*, 48:2426–2443, 2002.

[20] G. Modes. *Grundsätzliche Studie zur Populationsdynamik einer Extraktionskolonne auf Basis von Einzeltropfenuntersuchungen*. PhD thesis, Universität Kaiserslautern, 1999.

[21] X. Ni, D. Mignard, B. Saye, J. C. Johnstone, and N. Pereira. On the evaluation of droplet breakage and coalescence rates in oscillatory baffled reactor. *Chemical Engineering Sci.*, 57:2101–2114, 2002.

[22] E. A. Novikov and D. G. Dommermuth. Distribution of droplets in a turbulent spray. *Phys. Rev. E*, 56:5479–5482, 1997.

[23] S. V. Patankar. *Numerical Heat Transfer and Fluid Flow*. Hemisphere Pub., 1980.

[24] D. Ramkrishna. *Population balances*. Academic Press, 2000.

[25] D. Ramkrishna, A. Sathyagal, and G. Narishman. Analysis of dispersed-phase systems: fresh perspective. *AIChE Journal*, 41:35–44, 1995.

[26] A. E. Saez, M. A. Marquez, G. W. Roberts, and R. G. Carbonel. Hydrodynamic model for gas-lift reactors. *AIChE Journal*, 44:1413–1423, 1998.

[27] M. Sommerfeld. Validation of a stochastic lagrangian modelling approach for inter-particle collisions in homogeneous isotropic turbulence. *Int. J. Multiphase Flow*, 27:1829–1859, 2001.

[28] C. Tsouris and L. L. Tavlarides. Breakage and coalescence model for drops in turbulaent dispersions. *AIChE Journal*, 49:395–406, 1994.

[29] A. Vikhansky and M. Kraft. Single particle method for stochastic simulation of coagulation processes. Technical Report 14, c4e-Preprint Series, Cambridge, 2003.

[30] V. I. Vlasov. Impovement of the method of statistical trials (monte carlo) for calculation of rarefied gases flows. (in russian). *Doklady Akademii Nauk SSSR*, 167:1016–1018, 1966.

[31] T. von Karman and L. Horwarth. On the statistical theory of isotropic turbulence. *Proc. R. Soc. London*, A164:192–215, 1938.